Appl. Phys. B 88, 359–362 (2007)
DOI: 10.1007/s00340-007-2731-6
Applied Physics B
Lasers and Optics

Rapid communication

E. SMIRNOV[1]
C.E. RÜTER[1]
D. KIP[1,✉]
K. SHANDAROVA[2]
V. SHANDAROV[2]

Light propagation in double-periodic nonlinear photonic lattices in lithium niobate

[1] Institute of Physics and Physical Technology, Clausthal University of Technology, Leibnizstr. 4, 38678 Clausthal-Zellerfeld, Germany
[2] State University of Control Systems and Radioelectronics, 40 Lenin Ave., 634050 Tomsk, Russia

Received: 9 November 2006/Revised version: 16 April 2007
Published online: 19 July 2007 •

ABSTRACT Single- and double-periodic one-dimensional photonic lattices are formed in lithium niobate using both titanium in-diffusion and holographic grating recording. We investigate linear band structures and diffraction properties of such superlattices and observe a decrease of discrete diffraction with increasing modulation depth of the second superimposed lattice. In weakly modulated superlattices with tailored diffraction properties, our results demonstrate the formation of discrete solitons having a propagation constant inside the extra mini-gap formed inside the Brillouin zone.

PACS 42.65.Tg; 42.70.Qs; 42.82.Et

1 Introduction

Artificially structured dielectric materials, so-called meta-materials, possess many radically new optical properties. Here may be the most notable example is the vigorous search for negative index materials [1]. Another example of such artificial materials are one-(1D) and two-dimensional arrays of weakly coupled waveguides, which exhibit many new phenomena due to their unique diffraction properties arising from the evanescent coupling between adjacent channels [2–4]. Linear discrete diffraction in such waveguide arrays (WA) has led to the discovery of additional features such as anomalous and zero diffraction [5, 6], and light propagation in multiple allowed bands that are separated by forbidden gaps [3, 4, 7]. When higher light intensities are involved, a variety of nonlinear effects like discrete modulation instability [8, 9], formation of discrete solitons [10–14], and nonlinear interactions of such solitons allowing for all-optical switching and light steering have been demonstrated [15–17]. Recently, special attention has been paid to more complicated configurations of photonic lattices, for example modulated and quasi-periodic WAs [18, 19], and lattice interfaces [20, 21]. Especially the use of double-periodic lattices offers new degrees of freedom that allow one to engineer desirable band-gaps in the transmission spectrum and to tailor diffraction properties, and in this way, to design new soliton families in nonlinear media. Here a recent example is the study of matter wave gap soliton formation of Bose–Einstein condensates in optical superlattices [22, 23].

To study the properties of these photonic lattices in more detail, a promising way to form nonlinear superlattices is the use of photorefractive 1D WAs [13, 14, 24], which show a strong nonlinear response for light power in the microwatt range. In single-period permanent WAs, an additional, second refractive index modulation (grating) can be recorded holographically by two-beam interference. Alternatively, two or more gratings with different lattice periods may be recorded in planar waveguide layers. Such optically induced super-structures are more flexible with respect to permanent arrays and may be dynamically erased and reconfigured, thus allowing for advanced all-optical switching devices. In this work we put forward such a concept of optical induction of superlattices in photorefractive lithium niobate ($LiNbO_3$) crystals and investigate the linear and nonlinear diffraction properties. In weakly modulated nonlinear lattices with tailored diffraction coefficients, our results demonstrate the formation of a narrow mini-gap soliton.

2 Experimental methods

For our experiments both planar waveguide samples (i.e., 1D homogeneous media) and 1D WAs are used. The x-cut $LiNbO_3$ substrates are doped with Fe (concentration $c_{Fe} = 2.5 \times 10^{25}\,m^{-3}$) to enhance their photorefractive properties. A 10 nm thick Ti film is evaporated and in-diffused for 2 h at 1000 °C in air. The single-mode character of the formed planar waveguide for TE polarized green light is verified by mode spectroscopy [19]. Alternatively, permanent WAs are formed by lithographic patterning of a 10 nm thick Ti layer into stripes with a width 4.4 μm and separated by 4 μm [17]. Finally, the facets of the samples are polished for light coupling. One-dimensional single- and double-periodic WAs can be formed in the fabricated planar waveguides by two-beam holographic recording of one or two elementary gratings, respectively: each refractive index maximum of the modulated pattern forms

✉ Fax: +49-5323-72-2175, E-mail: d.kip@pe.tu-clausthal.de

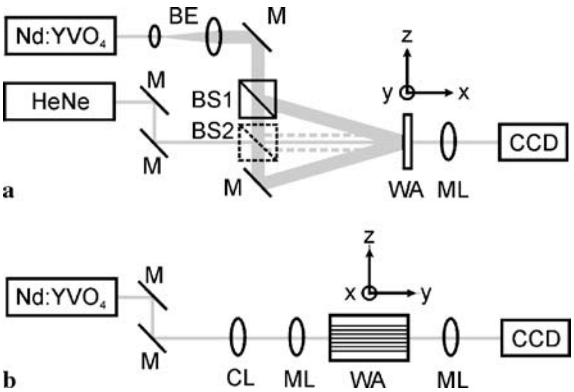

FIGURE 1 Experimental setups. (**a**) Recording scheme with M: mirror; BS, beam splitter; BE, beam expander; ML, microscope lens; CL, cylindrical lens; WA, waveguide sample; CCD, camera. (**b**) Single channel excitation for observation of discrete diffraction and soliton formation

a channel waveguide that is evanescently coupled to its next neighbors. Alternatively, a double-periodic superlattice can be realized by superimposing a holographic grating on a permanent, Ti in-diffused WA. In all cases grating vectors are aligned parallel along the z-direction, thus modulating the refractive index perpendicular to the light propagation direction along y. In the recording setup in Fig. 1a ordinarily polarized light of wavelength $\lambda = 532\,\mathrm{nm}$ is expanded and split into three mutually coherent beams that intersect inside the sample. With one of the beams blocked, each pair of beams generates an interference pattern $I(z) = I_0[1 + m\cos(2\pi z/\Lambda)]$ within the sample, where $I_0 = I_1 + I_2$ is the total intensity, m is the modulation, and $\Lambda = \lambda/(2\sin\theta)$ is the grating period, with 2θ being the full angle of two intersecting recording beams. Grating periods $\Lambda = (8–40)\,\mu\mathrm{m}$ can be selected by properly adjusting 2θ. By varying the exposure time t_r of the sample the refractive index amplitude Δn_g of the optically induced refractive index gratings can be adjusted in a range from $\approx 10^{-5}$ to 5×10^{-4} (for extraordinarily polarized light). Using two successive recordings, the resulting refractive index pattern of a superlattice with grating periods Λ and $N\Lambda$ ($N = 2, 3, ...$) is described by $\Delta n(z) = \Delta n_{g,1}\cos^2(\pi z/\Lambda) + \Delta n_{g,2}\cos^2(\pi z/(N\Lambda) + \varphi_0)$. Here φ_0 denotes the relative phase shift of the two gratings, which is adjusted to $\varphi_0 = 0$ by imaging the interferences patterns of each beam pair on the sample surface onto a CCD camera. In permanent WAs the phase contrast of the refractive index pattern is directly visible on the CCD camera, too. In this case the (weak) diffraction pattern formed behind the samples when a He-Ne laser illuminates the permanent grating is used to align additional holographic gratings in parallel.

3 Band structure and discrete diffraction

The linear modes of a 1D lattice are extended Floquet–Bloch (FB) modes, where the allowed propagation constants determine the band spectrum (dispersion relation) which consists of allowed bands and forbidden gaps. On the other hand, in a 1D planar waveguide layer free transverse propagation of modes results in a continuous spectrum with nearly parabolic shape, analogue to the propagation of free electrons. The dispersion relation $\beta(k_z)$ can be measured by excitation of pure FB modes using a modified prism coupler set-up [19]. As an example, in Fig. 2a, we show an intuitive experimental comparison of the dispersion of a planar waveguide layer (triangles) and a 1D single-period WA (squares). This is done by first optically recording an index grating ($\Lambda = 8\,\mu\mathrm{m}$, $t_r = 40\,\mathrm{min}$, $I_0 = 150\,\mathrm{mW/cm^2}$) in a planar waveguide followed by the band structure measurement. Here a band gap appears between the 1st and 2nd band, where the size of this gap is directly related to the amplitude Δn_g of the written index grating. Then this index pattern is optically erased by incoherent white light illumination, and the parabolic dispersion of the planar layer that is left after erasure is obtained when repeating the measurement.

Examples of different excited FB modes imaged from the sample's rear facet are given in Fig. 2b. Here 1 and 2 denote modes of the 1st and 2nd band, whereas A stands for the center of the Brillouin zone (BZ) ($k_z = 0$) while B represents the edge of BZ ($k_z = \pi/\Lambda$). Mode 2A in the center of the 2nd band is hardly guided because here $n_{\mathrm{eff}} - n_{\mathrm{sub}} < 0$. Comparison of the two photographs on the right-hand side nicely demonstrates the lateral shift of intensity maxima of mode 2B at the BZ edge by $\Lambda/2$ relative to mode 1B. This proves that light in mode 2B is guided mainly in-between channels. Unfortu-

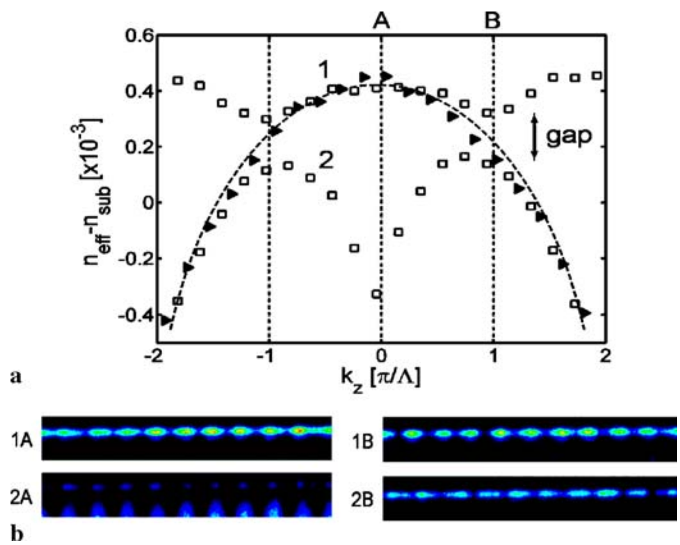

FIGURE 2 Measured band structure and FB modes of planar waveguide and 1D WA. (**a**) Effective refractive indices $n_{\mathrm{eff}} = \lambda\beta/2\pi$ vs. transverse wave vector k_z for (i) TE_0 modes of planar waveguide (*triangles*), and (ii) FB modes of 1st and 2nd transmission bands of a 1D WA with $\Lambda = 8\,\mu\mathrm{m}$ (*squares*). Values n_{eff} are given relative to the substrate index n_{sub}. (**b**) Intensity of excited FB modes on the sample's rear facet: 1A and 2A, center of BZ of 1st and 2nd band, respectively; 1B and 2B, edge of BZ of 1st and 2nd band, respectively

nately, the prism method [19] fails to clearly monitor the additional mini-gap formed in double-periodic lattices because of limited resolution. However, mini-gaps can be observed qualitatively when monitoring the light intensity on the rear sample facets of double-periodic lattices: For a superlattice with $N = 2$ a transformation of FB modes (similar to the change from 1B to 2B in Fig. 2b) is observed for modes launched with the (expected) transverse wave vector $k_z \approx \pi/2\Lambda$.

Next, we investigate the diffraction properties of a permanent WA that is additionally periodically modulated by a superimposed holographically recorded grating. This is done by coupling an extraordinarily polarized light beam into a single channel (at normal incidence, i.e., $k_z = 0$) via the input facet of the sample and inspecting the discrete diffraction pattern on the rear facet (see Fig. 1b). Here the input power is low ($P_{\text{in}} \approx 1\ \mu\text{W}$) and images are taken immediately after switching on the input light, so as to avoid any nonlinear effects. Furthermore, we perform numerical simulations based on a $(1+1)$D beam propagation method (BPM). We use a superlattice with parameters $\Lambda = 8.8\ \mu\text{m}$, $\Delta n_{\text{g},1} = 5.4 \times 10^{-3}$, $N = 3$, and $\Delta n_{\text{g},2} = 5 \times 10^{-4}$. In Fig. 3 the results of discrete diffraction are shown, where the left-hand side corresponds to excitation of a single channel with maximum refractive index change ("channel A", index changes of the two gratings add up), whereas the right-hand side corresponds to single-channel excitation of the next neighbored waveguide ("channel B") with smaller index maximum. Obviously, in the first case "A" diffraction is rather weak and coupling occurs to next neighbors only. On the other hand, for case "B", strong discrete diffraction is observed, where the intensity spectrum on the rear facets has a similar width as compared to the one for single-periodic (permanent) lattices.

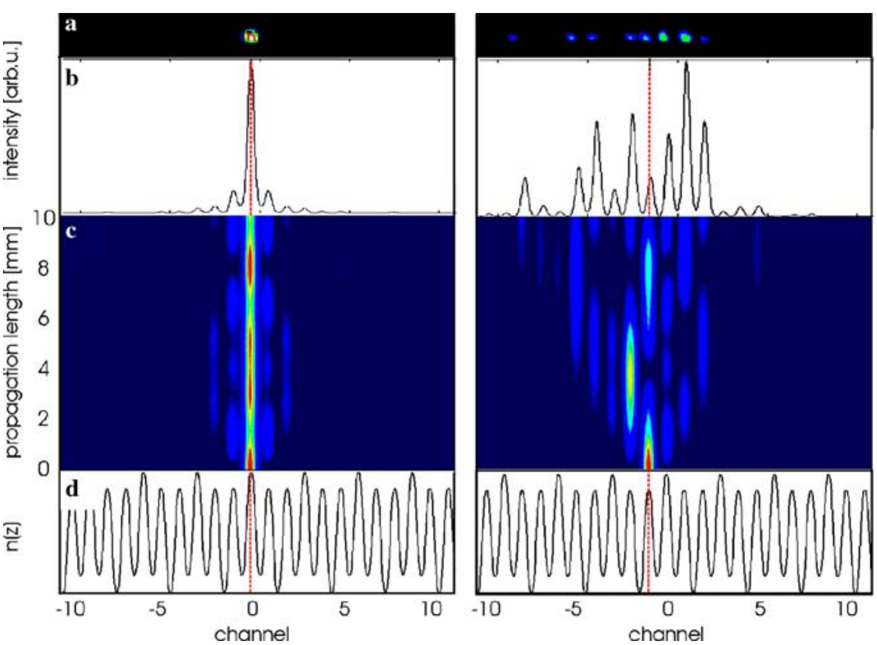

FIGURE 3 Discrete light diffraction in double-periodic lattices for single channel excitation (see text). (**a**) measured intensity distribution on rear facet; (**b,c**) linear BPM simulation of light propagation, with (**b**) output intensity profile, and (**d**) corresponding refractive index profile of the superlattice. *Vertical dotted lines* mark the excited channel

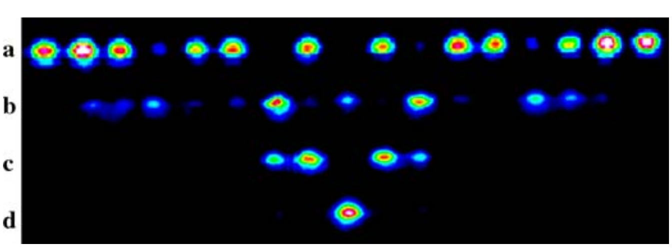

FIGURE 4 Discrete diffraction in a double-periodic lattice with $\Lambda = 8.8\ \mu\text{m}$, $\Delta n_{\text{g},1} = 5.4 \times 10^{-3}$, $N = 3$, and different recording times t (different $\Delta n_{\text{g},2}$). Single-channel excitation of channel A for (**a**) $t = 0$; (**b**) $t = 3$ min; (**c**) $t = 5$ min; (**d**) $t = 15$ min

In Fig. 4 we investigate linear discrete diffraction for excitation of channel A in double-periodic lattices with different strength $\Delta n_{g,2}$ of the additional modulation. This is achieved by using different recording times of the photorefractive grating (3 min, 5 min, and 15 min, where the latter corresponds to $\Delta n_{\text{g},2} \approx 5 \times 10^{-4}$). Starting from the single-periodic lattice diffraction decreases for an increase of $\Delta n_{\text{g},2}$, and for $t_{\text{r}} = 15$ min coupling of light to neighbored channels is almost completely suppressed. Thus, we can easily control the diffraction characteristics of optically induced double-periodic WAs by changing the parameters of the recording process. We want to note that diffraction patterns totally reconstruct when shifting the narrow input beam by $N = 3$ channels.

4 Formation of mini-gap solitons

A standard experiment of light propagation in a nonlinear photonic lattice or WA is the formation of a localized optical state or discrete soliton. Because the nonlinearity in $LiNbO_3$ is of the defocusing (negative) type, such a soliton can be formed at the BZ edge of the 1st band, where the diffraction coefficient is positive (anomalous diffraction). Consequently, the propagation constant of the nonlinear wave is decreased and located inside the gap. The corresponding Floquet–Bloch modes have an alternating (staggered) phase profile; thus, the soliton is called a staggered gap soliton [13, 14].

In a double-periodic lattice, the additional modulation leads to the formation of an extra gap inside the BZ of the 1st lattice. This gap is formed at a transverse wave vector $k_z = \pi/(N\Lambda)$. Due to the small additional modulation used here (the amplitude of the holographically written grating is at least one order of magnitude lower than the permanent one), the size of this extra gap is small, thus it may be called a mini-gap.

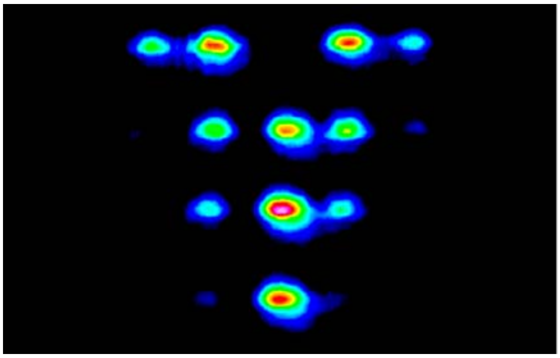

FIGURE 5 Formation of mini-gap soliton in a double-periodic 1D WA using $P_{\mathrm{in}} = 5\,\mu\mathrm{W}$

In single-periodic WAs, it has been demonstrated that gap solitons can be formed by excitation of a single input channel [17, 25]. In the linear case, the narrow input wave excites a spectrum of FB modes with transverse wave vectors around $k_z = \pi/\Lambda$ (BZ edge). With an appropriate nonlinearity involved, such input excitation may form a staggered gap soliton with a propagation constant in the finite gap between 1st and 2nd band. In case of a double-periodic lattice, single-channel excitation of channel A or B has to be distinguished. Here channel B is related to the single-periodic situation (i.e., excitation of waves at $k_z \approx \pi/\Lambda$), whereas excitation of channel A corresponds to FB modes with a spectrum of transverse wave vectors around $k_z = \pi/(N\Lambda)$. Consequently, when such a WA possesses a defocusing nonlinearity, a soliton inside the additional mini-gap may form. Because diffraction of light for excitation of channel A is lower when compared to case B, also the required nonlinearity for mini-gap soliton formation is reduced.

Figure 5 monitors the build-up of a discrete mini-gap soliton in a double-periodic WA (see Fig. 4c) with $N = 3$. Because of the photorefractive nonlinearity and the still low input power, the soliton build-up time is rather slow. Therefore we can monitor the temporal development by imaging the output intensity on the CCD camera. The initial image at $t = 0$ shows linear discrete diffraction. With increasing time the output distribution becomes narrower, and finally at $t = 90\,\mathrm{s}$ forms a narrow mini-gap soliton where the energy is mainly localized in one channel. This structure is stable for times large compared to the build-up time constant. For comparison, using the same optical input power (i.e., the same optical nonlinearity), we repeated the experiment but now excited a single channel of type B. For this case only partial focusing of the output light to about 5 channels is observed. On the other hand, if the input power of channel B is significantly increased by a factor ≈ 3, a "normal" gap soliton is formed [21].

5 Conclusions

In conclusion, we have demonstrated the optical induction of single-period WAs and superlattices in photorefractive $LiNbO_3$ crystals. Weakly modulated superlattices are formed by superposition of permanent WAs fabricated by Ti in-diffusion and holographic gratings. We have shown that diffraction properties can be tailored by adjusting grating period and strength of the superimposed grating. For the first time to the best of our knowledge, we have experimentally observed suppression of discrete diffraction in strongly modulated double-periodic superlattices as well as formation of mini-gap solitons in superlattices with weak additional modulation.

ACKNOWLEDGEMENTS We acknowledge financial support from German BMBF (DIP-E6.1) and DFG (KI482/11-1), and Russian RFBR (06-02-39017).

REFERENCES

1 D.R. Smith, J.B. Pendry, M.C.K. Wiltshire, Science **305**, 788 (2004)
2 D.N. Christodoulides, R.I. Joseph, Opt. Lett. **13**, 794 (1988)
3 D.N. Christodoulides, F. Lederer, Y. Silberberg, Nature **424**, 817 (2003)
4 J.W. Fleischer, G. Bartal, O. Cohen, T. Schwartz, O. Manela, B. Freedman, M. Segev, H. Buljan, N.K. Efremidis, Opt. Express **13**, 1780 (2005)
5 H.S. Eisenberg, Y. Silberberg, R. Morandotti, J.S. Aitchison, Phys. Rev. Lett. **85**, 1863 (2000)
6 P.T. Rakich, M.S. Dahlem, S. Tandon, M. Ibanescu, M. Soljacic, G.S. Petrich, J.D. Joannopoulos, L.A. Kolodziejski, E.P. Ippen, Nature Mater. **5**, 93 (2006)
7 C.E. Rüter, J. Wisniewski, D. Kip, Opt. Lett. **31**, 2768 (2006)
8 J. Meier, G.I. Stegeman, D.N. Christodoulides, Y. Silberberg, R. Morandotti, H. Yang, G. Salamo, M. Sorel, J.S. Aitchison, Phys. Rev. Lett. **92**, 163 902 (2004)
9 M. Stepić, C. Wirth, C.E. Rüter, D. Kip, Opt. Lett. **31**, 247 (2006)
10 H.S. Eisenberg, Y. Silberberg, Y. Morandotti, R. Boyd, J.S. Aitchison, Phys. Rev. Lett. **81**, 3383 (1998)
11 J.W. Fleischer, T. Carmon, M. Segev, N.K. Efremidis, D.N. Christodoulides, Phys. Rev. Lett. **90**, 023 902 (2003)
12 D.N. Neshev, E. Ostrovskaya, Y.S. Kivshar, W. Królikowski, Opt. Lett. **28**, 710 (2003)
13 D. Mandelik, R. Morandotti, J.S. Aitchison, Y. Silberberg, Phys. Rev. Lett. **92**, 093 904 (2004)
14 F. Chen, M. Stepić, C.E. Rüter, D. Runde, D. Kip, V. Shandarov, O. Manela, M. Segev, Opt. Express **13**, 4314 (2005)
15 D.N. Christodoulides, E.D. Eugenieva, Phys. Rev. Lett. **87**, 233 901 (2001)
16 J. Meier, G.I. Stegeman, Y. Silberberg, R. Morandotti, J.S. Aitchison, Phys. Rev. Lett. **93**, 093 903 (2004)
17 M. Stepić, E. Smirnov, C.E. Rüter, L. Prönneke, D. Kip, V. Shandarov, Phys. Rev. E **74**, 046 614 (2006)
18 C.R. Rosberg, I.L. Garanovich, A.A. Sukhorukov, D.N. Neshev, W. Królikowski, Y.S. Kivshar, Opt. Lett. **31**, 1498 (2006)
19 A.A. Sukhorukov, Phys. Rev. Lett. **96**, 113 902 (2006)
20 S. Suntsov, K.G. Makris, D.N. Christodoulides, G.I. Stegeman, A. Haché, R. Morandotti, H. Yang, G. Salamo, M. Sorel, Phys. Rev. Lett. **96**, 063 901 (2006)
21 E. Smirnov, M. Stepić, C.E. Rüter, D. Kip, V. Shandarov, Opt. Lett. **31**, 2338 (2006)
22 S. Peil, J.V. Porto, B.L. Tolra, J.M. Obrecht, B.E. King, M. Subbotin, S.L. Rolston, W.D. Phillips, Phys. Rev. A **67**, 051 603 (2003)
23 P.J.Y. Louis, E.A. Ostrovskaya, Y.S. Kivshar, Phys. Rev. A **71**, 023 612 (2005)
24 D. Kip, Appl. Phys. B **67**, 131 (1998)
25 M. Matuszewski, C.R. Rosberg, D.N. Neshev, A.A. Sukhorukov, A. Mitchell, M. Trippenbach, M.W. Austin, W. Krolikowski, Y.S. Kivshar, Opt. Express **14**, 254 (2006)